SUPPLEMENTARY INFORMATION

Virus-induced cell gigantism and asymmetric cell division in Archaea

Short title: Cell cycle manipulation by an archaeal virus

Junfeng Liu[a,b], Virginija Cvirkaite-Krupovic[a], Diana P. Baquero[a], Yunfeng Yang[b], Qi Zhang[c], Yulong Shen[b]*, Mart Krupovic[a]*

[a] Archaeal Virology Unit, Institut Pasteur, 75015 Paris, France
[b] CRISPR and Archaea Biology Research Center, State Key Laboratory of Microbial Technology, Microbial Technology Institute, Shandong University, 266237 Qingdao, China
[c] Faculty of Life Science and Technology, Kunming University of Science and Technology, 650500 Kunming, China

* – Correspondence to:
Mart Krupovic
Archaeal Virology Unit,
Department of Microbiology, Institut Pasteur,
75015 Paris, France
E-mail: mart.krupovic@pasteur.fr

Yulong Shen
CRISPR and Archaea Biology Research Center,
State Key Laboratory of Microbial Technology,
Microbial Technology Institute,
Shandong University,
266237 Qingdao, China
E-mail: yulgshen@sdu.edu.cn

This PDF contains
Supplementary Methods
Supplementary Figures S1-S9
Legend for Supplementary video S1
Supplementary Table S1
Supplementary references

SI Methods

Propagation and purification of virus particles

STSV2 was propagated in *S. islandicus* REY15A. A stock of STSV2-infected REY15A cells was inoculated into TSV medium and incubated at 75°C with shaking. When the OD_{600} reached 0.6-0.8, the cell culture was transferred to 4 × 1L TSV medium containing mineral salt solution, 0.2% (wt/vol) tryptone (T), 0.2% (wt/vol) sucrose (S) and a mix of vitamins (V); the pH of medium was adjusted to 3.5 with sulfuric acid. When the OD_{600} reached ~0.8, the cells were removed by centrifugation at 7,000 rpm for 20 min. The supernatant containing STSV2 was first filtered with 0.45 μm filter to remove the remaining cells and cell debris, and then concentrated by the Vivaflow 200 Crossflow cassette (Sartorius Stedim Lab Ltd, Stonehouse, GL10 3UT, UK). STSV2 was further concentrated by ultracentrifugation at 35,000 rpm (Type 50.2 Ti rotor) for 2 h and then resuspended in mineral salt medium. The virus was further purified by sucrose gradient and CsCl gradient ultracentrifugation, and stocked at 4°C until used. Sulfolobus monocaudavirus 1 (SMV1) and Sulfolobus spindle-shaped virus 2 (SSV2) were propagated in the highly susceptible strain, *S. islandicus* CRISPR deletion mutant ΔC1C2 as described previously (1, 2). SMV1 and SSV2 were purified in a similar way as STSV2.

Plaque and spot assays

TS medium supplemented with 0.1% (wt/vol) yeast extract and 0.3% (wt/vol) phytagel was used for plaque assays. The titer of STSV2 was determined by plaque assays. Serial dilutions of the viral preparations (100 μL) were mixed with *S. islandicus* REY15A cells. Then 10 mL pre-heated TSY medium containing 0.3% phytagel was added to the mixture, vortexed and immediately poured into the empty Petri dishes. The plates were incubated at 75°C. After about 1.5 days, visible STSV2 plaques appeared as small clear halos.

For the spot assay, wild type REY15A cells and REY15A cells with different numbers of CRISPR spacers (S1, S2 and S3) were collected at mid-logarithmic phase and mixed with 10 ml of pre-heated TYS medium containing 0.3% (wt/vol) phytagel, vortexed and immediately poured into the empty Petri dishes. After the plates solidified, 5μl of the serially diluted STSV2 preparation were applied on the plates and incubated at 75 °C for 1.5 days.

Bright-field microscopy

5 μl of non-infected and infected cell cultures at indicated time points were examined under an inverted fluorescence microscope (Carl Zeiss, Germany) in differential interference contrast (DIC) mode.

Fluorescence microscopy

Fluorescence microscopy analysis was performed as previously described (3). Briefly, non-infected and STSV2-infected REY15A cells were collected and pelleted down at 6,000 rpm for 5 min, and resuspended in 300 μl PBS buffer (137 mM NaCl, 2.7 mM KCl, 10 mM $Na_2HPO_4 \times 12H_2O$, 2 mM KH_2PO_4). The cells were fixed by adding 700 μl of cold absolute ethanol at 4°C for 2 h. Then the cells were pelleted down and washed with PBST buffer (PBS plus 0.05% Tween-20) for 3 times at 6,000 rpm for 5 min. The primary antibody against ESCRT-III-1 (HuaAn Biotechnology Co., Hangzhou, Zhejiang, China) was added (dilution of 1:1000 in PBST buffer) and incubated at 4°C overnight. The cells were then pelleted down and washed with PBST buffer for 3 times at 6,000 rpm for 5 min. Goat anti-rabbit IGG Alexa Fluor® 568, Invitrogen™ (Thermo Fisher Scientific, USA) was added (dilution of 1:1000 in PBST) and incubated at room temperature for 2 h. Then the cells were pelleted down and washed with PBST buffer for 3 times at 6,000 rpm for 5 min. The cells were finally resuspended in PBS buffer containing BODIPY (Thermo Fisher Scientific, USA) and DAPI (4', 6-diamidino-2-phenylindole) to stain the membrane and DNA, respectively. After 30 min of staining, the samples were observed under a Leica TCS SP8 confocal microscope (Leica, Germany).

For 3D confocal imaging, the live cells from non-infected and STSV2-infected REY15A cultures were collected and pelleted down at 6,000 rpm for 5 min and then resuspended in PBS buffer containing DAPI.

After 30 min of staining, the samples were observed under a Leica TCS SP8 confocal microscope (Leica, Germany) with a z-step of about 0.35-0.45 μm. The 3D confocal series were reconstructed by Leica Application Suite X (LAS X) software (Leica). The 3D volume visualization was shown together with the depth coding to display the depth information. The 3D video was obtained by rotation around Y-axis and then the X-axis with 1.5 times enlargement.

Transmission electron microscopy

For negative-staining TEM analysis, 10 μl of virus preparations or virus-infected cells were adsorbed onto glow-discharged copper grids with carbon-coated Formvar film and negatively stained with 2.0% (w/v) uranyl acetate. The samples were then observed under FEI Tecnai BioTwin 120 microscope (FEI, Einthoven, The Netherlands) operated at 120 kV.

Scanning electron microscopy

Non-infected and STSV2-infected cell cultures were collected at the indicated times and the samples were prepared as described previously (4). The samples were then loaded onto SEM specimen stubs with double adhesive tape and sputter coated with gold. Microscopy analysis was performed under high vacuum mode with 5.0 Kv electron beam using the AURIGA Compact Focused Ion Beam Scanning Electron Microscope (Carl ZEISS, Germany).

Flow cytometry

Non-infected and STSV2 infected cells (approximately 3×10^7 CFU) were harvested at the indicated time points and fixed with 70% cool ethanol overnight (>12 h). The fixed cells were then collected by centrifugation at 675×*g* for 20 min and resuspended in 1 ml of PBS buffer (137 mM NaCl, 2.7 mM KCl, 10 mM $Na_2HPO_4 \times 12H_2O$, 2 mM KH_2PO_4, pH 7.4,) with 0.05% Tween-20. The cells were precipitated again and resuspended in 100 μl of staining buffer containing 40 μg/ml propidium iodide (PI). After staining for at least 30 min, the samples were analyzed for DNA content using the Amnis® ImageStreamX Mark II imaging flow cytometer (Merck Millipore, Germany). The data of 100,000 imaged cells or particles were collected from each sample and then single cells were selected and analyzed for DNA content by IDEAS data analysis software.

For sorting of the STSV2-infected cell population into populations of different sizes, MoFlo Astrios cell sorter (Beckman Coulter) was used. The sorting was carried out with a 70 μm nozzle at a pressure of 60 PSI and a differential pressure with the sample of 0.3-0.4 PSI. The calibration of the machine was carried out using Megamix-Plus SSC beads (BioCytex).

Quantitative reverse transcription PCR (RT-qPCR)

Samples from non-infected and STSV2-infected REY15A cells were collected at the indicated time points, and the total RNAs were extracted using TRI Regent (SIGMA-Aldrich, USA). The quality and quantity of the total RNAs were checked using the Eppendorf BioSpectrometer basic (Eppendorf AG, Germany) and agarose (1%) gel electrophoresis.

Quantitative reverse transcription PCR (RT-qPCR) was carried out to determine the transcriptional levels of the cell division genes during the infection process. First-strand cDNAs were synthesized from the total RNAs according to the protocol from the Maxima First Strand cDNA Synthesis Kit for RT-qPCR with dsDNase (Thermo Scientific, USA). The resulting cDNA preparations were used to evaluate the mRNA levels of the cell division proteins by qPCR, using Luna Universal qPCR Master Mix (New England Biolabs, USA) and gene specific primers (Table S1). PCR was performed in an Eppendorf MasterCycler RealPlex^4 (Eppendorf AG, Germany) with the following steps: denaturing at 95°C for 2 min, 40 cycles of 95°C 15 s, 55°C 15 s and 68°C 20 s. Relative amounts of mRNAs were evaluated using the comparative Ct method with 16S rRNA as the reference (5).

PCR amplification of the CRISPR loci

Leader proximal regions (~750 bp) of the two CRISPR loci, extending from the leader sequence to the fifth spacer (-432 to 231 for locus 1 and -424 to 239 for locus 2) were amplified. Genomes from the non-infected and STSV2-infected REY15A cells at indicated time points were extracted and 100 ng of the purified DNA were used as templates for PCR amplification. The primers used for PCR are listed in Table S1. PCR was performed using Phusion DNA polymerase (Thermo Fisher Scientific, USA) with the following steps: denaturation at 98℃ for 10 min, 20 cycles of 98℃ 10 s, 50℃ 20 s and 72℃ 1 min.

SI Figures and legends

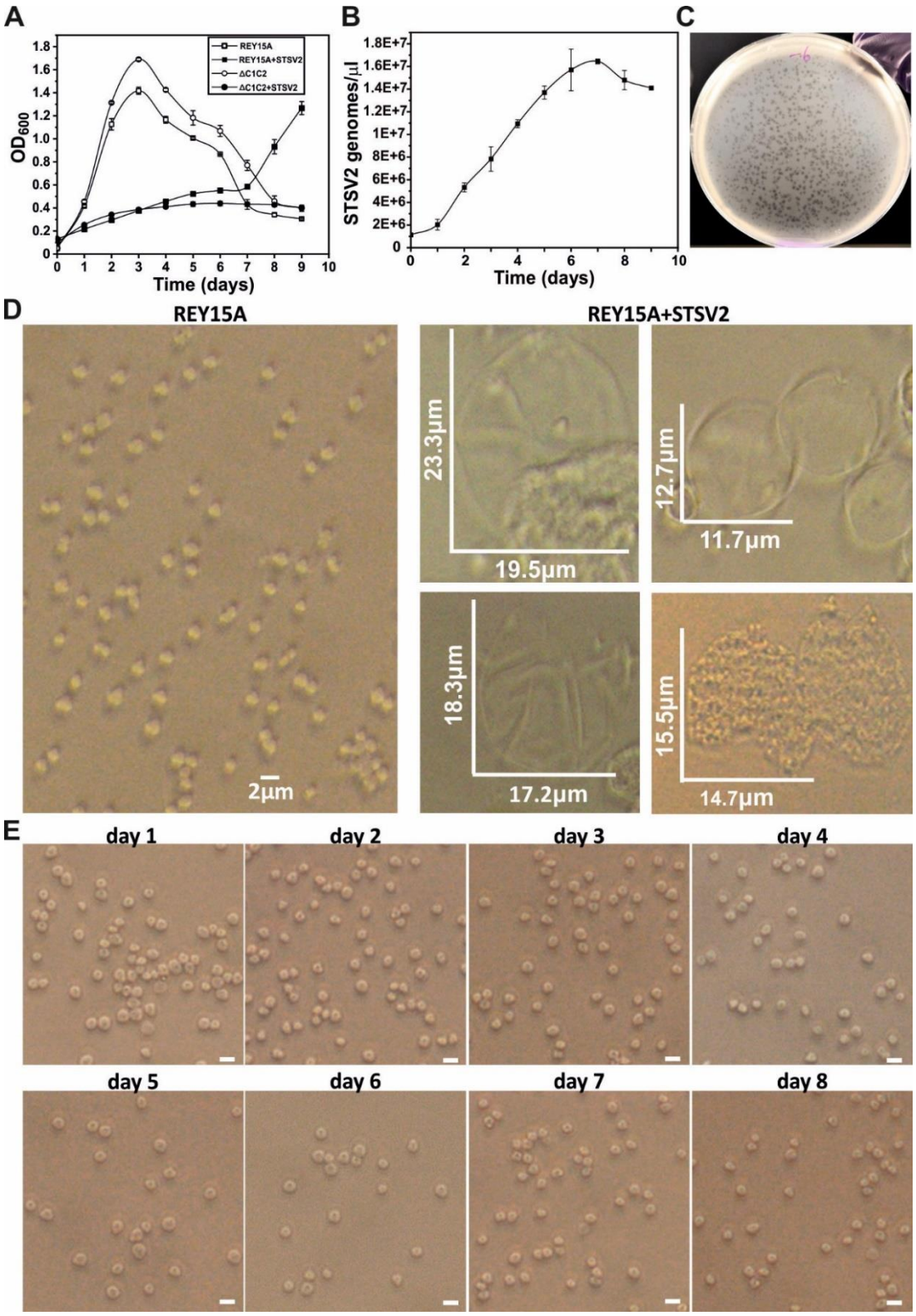

Figure S1. STSV2 infection induces growth retardation but no lysis. (A) Growth curves of non-infected and STSV2-infected REY15A and ΔCRISPR (ΔC1C2) cells. Error bars represent standard deviation from

three independent experiments. The cells were infected using a multiplicity of infection of 10. (B) Enumeration of extracellular STSV2 virions over the course of 9 days. The infected cell cultures were collected at the indicated time points and the cells were removed by centrifugation (7,000 rpm for 10min), whereas 1 μl of the supernatant was used as the template for qPCR. Error bars represent standard deviation from three independent experiments. (C) Plaque assay. Representative image of the STSV2 plaques formed on the plate of REY15A cells. The plaque assay was carried out as described in Material and Methods. The plaques are a manifestation of the slower growth of infected cells compared to the surrounding non-infected cells. (D) Representative images of the STSV2-infected giant cells. Left, non-infected REY15A cells; right, STSV2-infected REY15A cells with different sizes. The cell sizes are indicated with the corresponding scale bars. (E) Bright-field microscopy analysis of non-infected REY15A cells over the course of 8 days. There was no obvious change in the cell size during the time of experiment for non-infected cells. Bars, 2 μm.

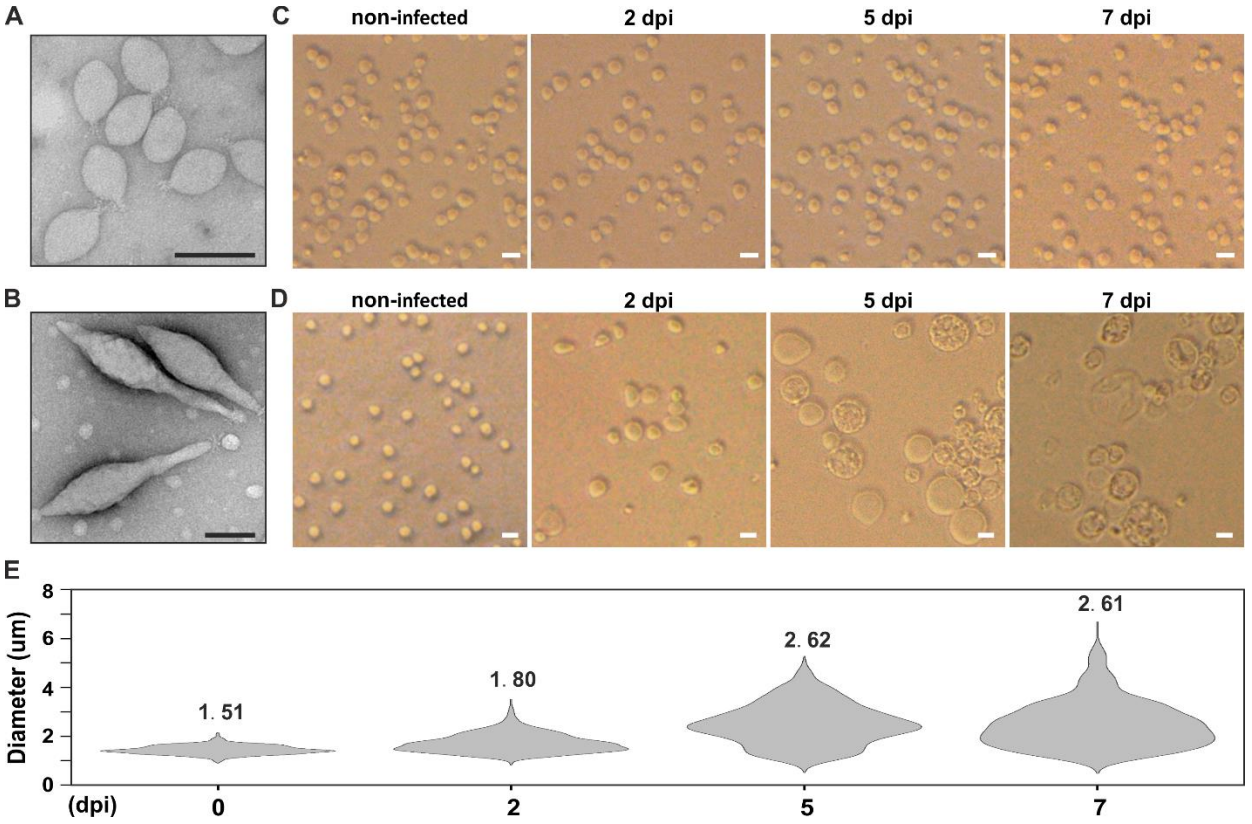

Figure S2. Effect of SSV2 and SMV1 on the size of *S. islandicus* ΔC1C2 cells. (A) Transmission electron micrograph of SSV2 virions negatively stained with 2.0% (w/v) uranyl acetate. Scale bar, 100 nm. (B) Transmission electron micrograph of SMV1 virions negatively stained with 2.0% (w/v) uranyl acetate. Scale bar, 100 nm. (C) Bright-field microscopy analysis of non-infected and SSV2-infected *S. islandicus* ΔC1C2 cells. SSV2 infection does not induce appreciable changes in cell size. Scale bars, 2 μm. (D) Bright-field microscopy analysis of non-infected and SMV1-infected *S. islandicus* ΔC1C2 cells. Similar to STSV2, SMV1 infection induces the formation of abnormally big cells. Scale bars, 2 μm. (E) Size distribution of the SMV1-infected ΔC1C2 cells during different time points after infection. The numbers above the plots represent median diameters of cells during each time point. dpi, days post infection.

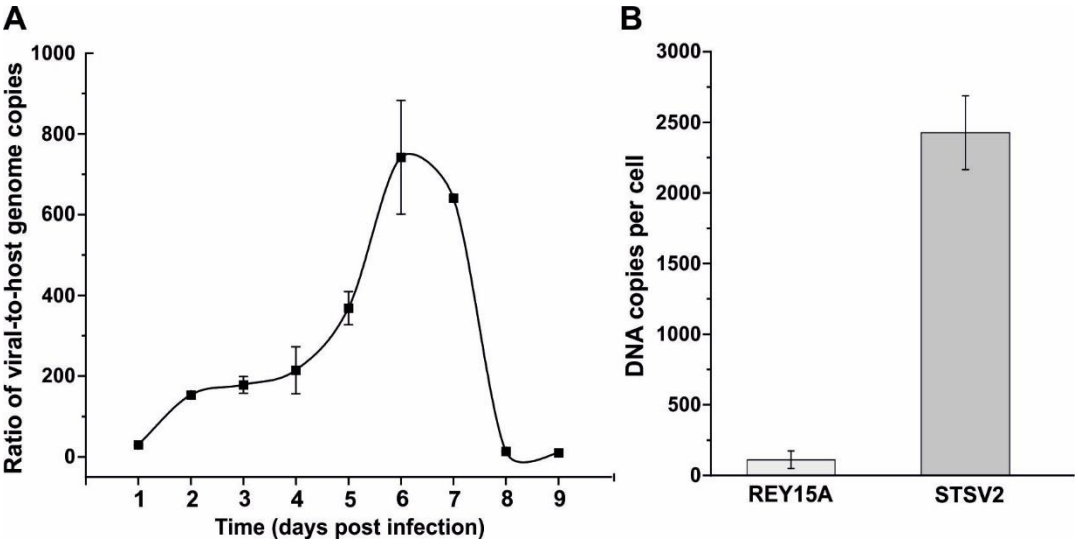

Figure S3. qPCR analysis of the viral and host DNA copy numbers in the infected cells. (A) Ratio of viral-to-host genome copies in STSV2 infected cells. STSV2-infected REY15A cells were collected at different time points post infection, the total (viral + cellular) DNA was extracted and used as a template for qPCR with chromosome (ESCRT-III-3-F/R; Table S1)- and virus (STSV2_37-F/R; Table S1)-specific primers. Plotted is the ratio between the copy numbers of the viral and cellular genomes. The error bars represent standard deviation from three independent experiments. (B) Quantification of the viral and host DNA copy numbers per cell by qPCR. The infected big cells at 6 dpi with a diameter more than 5 μm (from 6 to 16 μm, median 9.45 μm) were sorted by flow cytometry and 1,000 cells were used as the template for qPCR. Error bars represent standard deviation from three independent experiments.

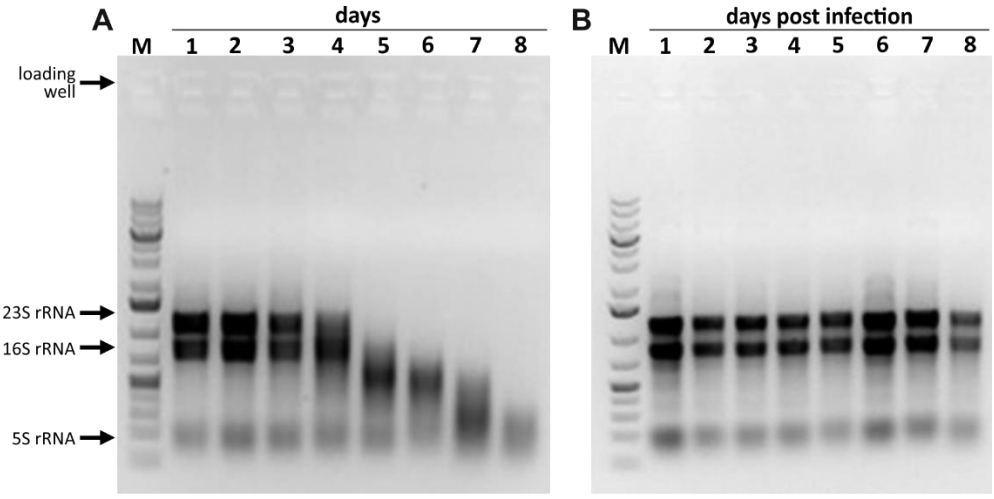

Figure S4. Determination of the quality of the RNA extracted from the non-infected (A) and STSV2-infected (B) REY15A cells. Once the non-infected cells entered the death phase (day 4), the RNA started to degrade (A). By contrast, no degradation of the RNA was observed in the STSV2-infected cells (B). M, molecular size marker.

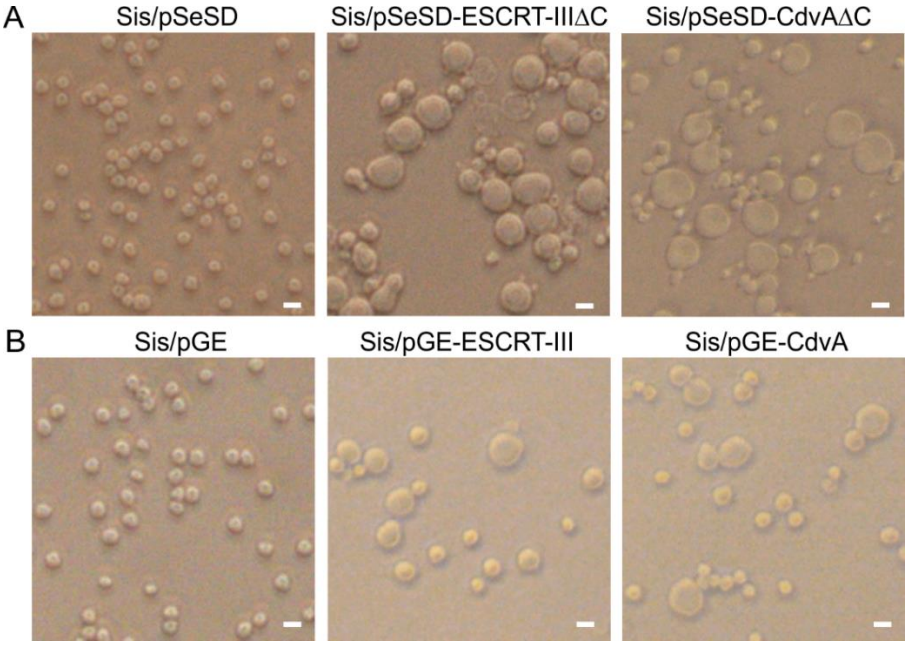

Figure S5. Overexpression of defective cell division proteins and transcriptional repression of cell division genes leads to appearance of cells with large diameters. (A) Bright-field micrographs of *S. islandicus* (Sis) cells carrying the empty pSeSD vector (control; left) as well as plasmids pSeSD-ESCRT-IIIΔC (middle) and pSeSD-CdvAΔC (right) expressing C-terminally truncated proteins ESCRT-III and CdvA, respectively. Cells with diameters of 4-5 μm can be observed in the case of both overexpression plasmids. Bars, 2 μm. (B) Bright-field micrographs of *S. islandicus* (Sis) cells carrying the empty pGE vector (control; left) as well as plasmids pGE-ESCRT-III (middle) and pGE-CdvA (right) carrying CRISPR spacers targeting transcripts of genes encoding ESCRT-III and CdvA, respectively. Cells with diameters of 4 μm can be observed in the case of both plasmids. Bars, 2 μm.

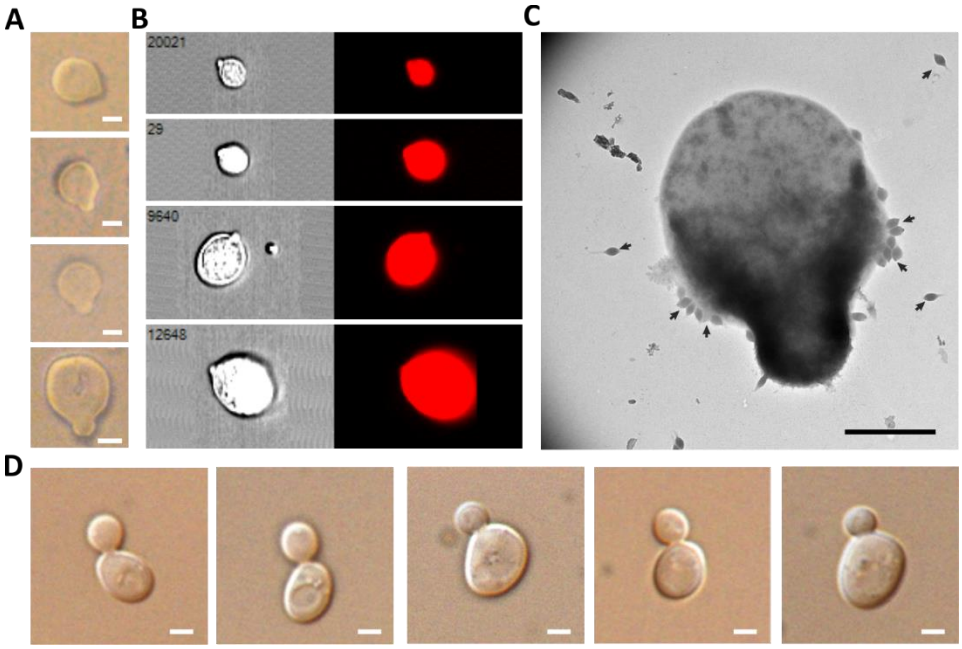

Figure S6. Asymmetric cell division by budding. (A-C) Representative images of asymmetrically dividing REY15A cells infected by STSV2 observed by bright-field microscopy (A), fluorescence microscopy following cell sorting by flow cytometry (B) and transmission electron microscopy (C). STSV2 virions attached to the cell surface are indicated with black arrows in panel C. Scale bars, 1 μm. (D) A selection of bright-field micrographs of asymmetrically dividing budding yeast. Scale bars, 2 μm.

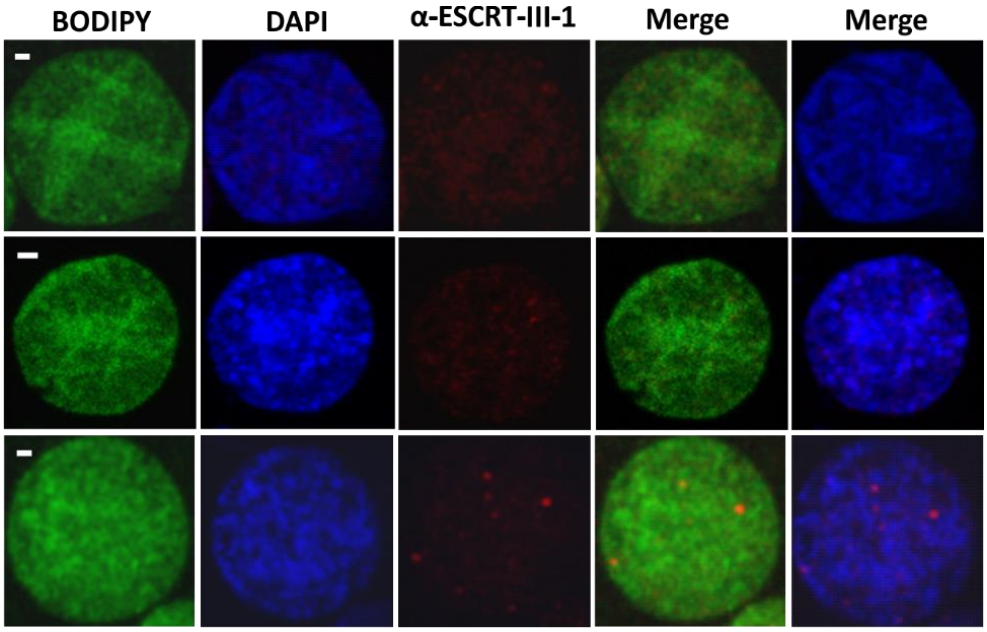

Figure S7. Fluorescence microscopy analysis of the STSV2-infected giant *S. islandicus* cells. In the absence of asymmetric division by budding, ESCRT-III-1 forms only small dot-like foci, rather than ring or spiral-like structure observed in the presence of the budding cells. Fixed cells were stained with BODIPY (green) to visualize the membrane, DAPI (blue) to visualize DNA and fluorescently labelled anti-ESCRT-III-1 antibody (red) to visualize ESCRT-III-1. Scale bars, 1 μm.

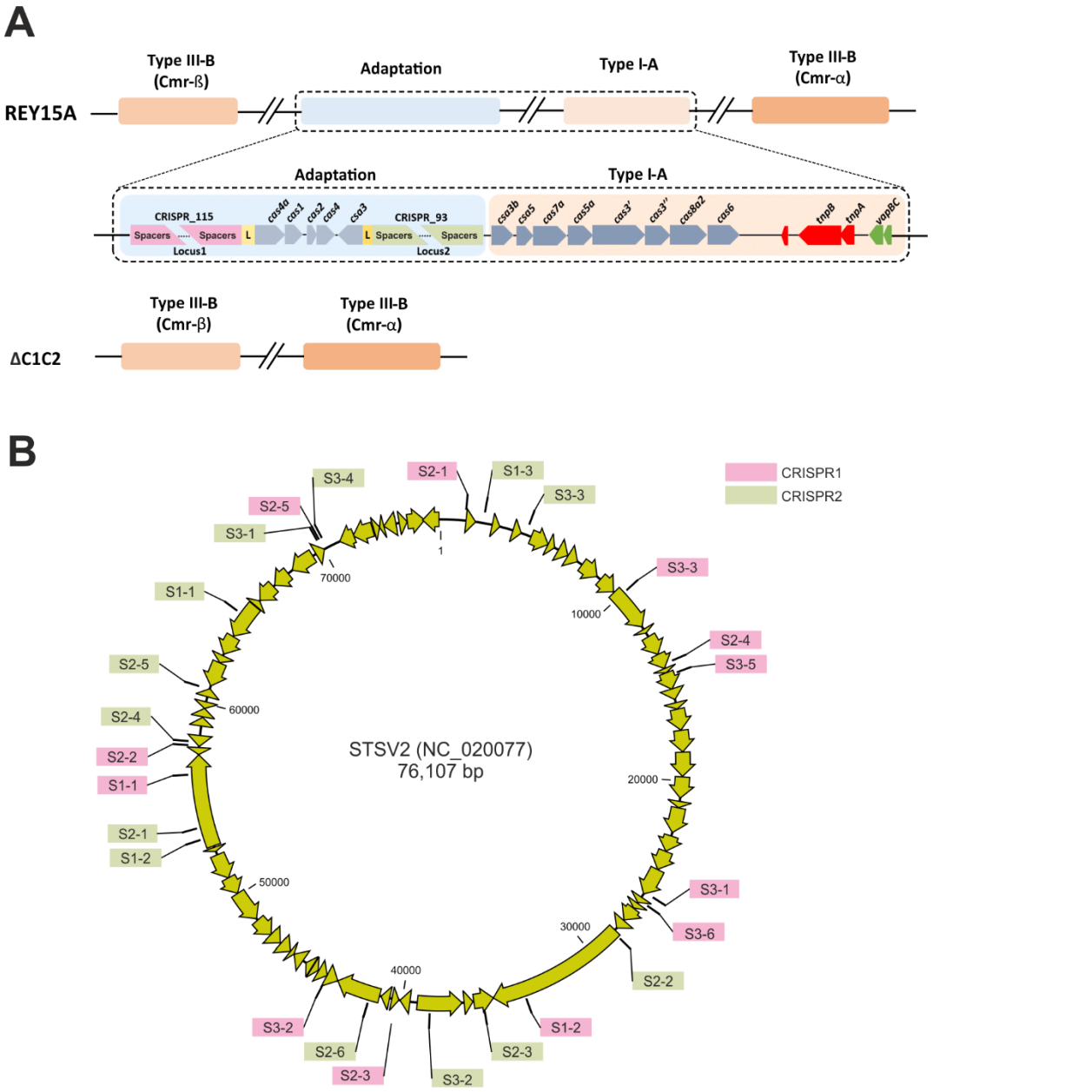

Figure S8. Development of CRISPR-dependent resistance to STSV2. (A) Overview of the CRISPR-Cas loci in *S. islandicus* REY15A (top). ΔC1C2 (bottom) is a deletion mutant, which lacks the only adaptation module, including the two CRISPR loci (pink and green, respectively), and the Type I-A interference module. L, leader sequence. (B) Distribution of the protospacers targeted by spacers present in the three STSV2-resistant REY15A strains, S1–S3. Protospacers found in the CRISPR1 and CRISPR2 loci are shown on the pink and green backgrounds, respectively.

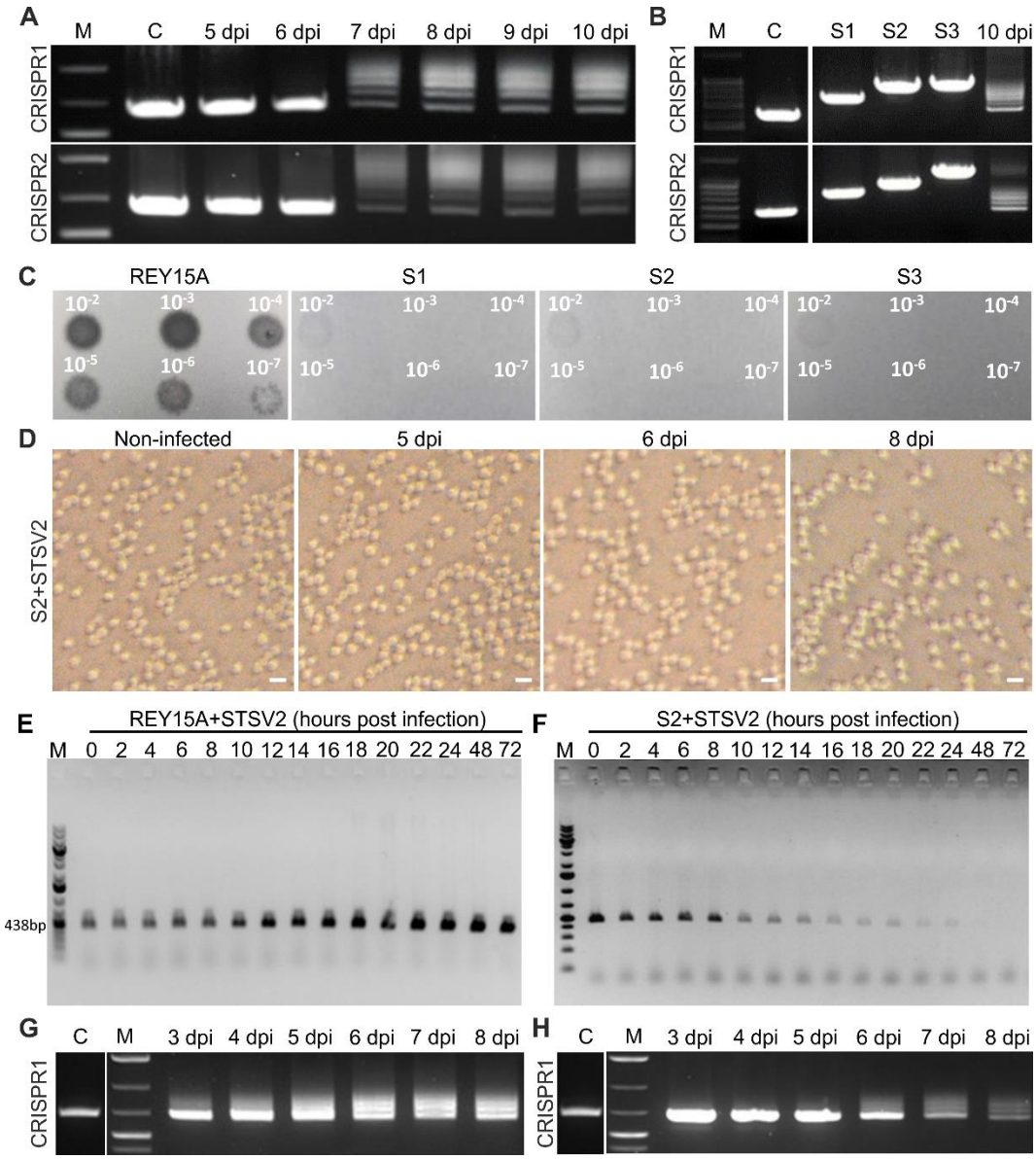

Figure S9. STSV2-infected cells develop CRISPR-based resistance. (A) Acquisition of new CRISPR spacers by STSV2-infected REY15A cells. Agarose gels show PCR products of the leader-proximal repeat-spacer units amplified from the cultures of infected cells at different time points using specific primers complementary to the leader sequence (forward primer) and the fifth spacer of the parental strain (reverse primer; Table S1). Two pairs of primers were used to amplify spacers acquired in the CRISPR loci (CRISPR1 and CRISPR2, respectively). C, positive control (PCR product obtained using the non-infected REY15A strain as a template); M, molecular size marker; dpi, days post infection. (B) Spacer content of the 3 purified clones, S1-S3, resistant to STSV2 infection. PCR amplification was performed as described in panel A. Last lane for both CRISPR1 and CRISPR2 loci shows the amplification products from the 10 dpi culture. (C) Spot test on the lawns of the parental REY15A strain and the 3 purified clones, S1-S3, resistant to STSV2 infection and carrying variable numbers of spacers. (D) Bright-field microscopy analysis of the S2 cells infected with STSV2. Scale bars: 2 μm. (E, F) PCR amplification of the STSV2 genome in REY15A cells without (E) and with (F) CRISPR spacers (S2). Around 0.7×10^8 infected cells were collected, pelleted and washed 3 times with fresh medium (7,000 rpm, 10 min) to remove the extracellular

virus particles. Finally, the cells were re-suspended in 400 µl of fresh medium and 2 µl were used as a template for PCR with the primers specifically targeting the gene encoding the coat protein (STSV2_37-F/R; Table S1) of the virus. (G,H) Spacer content of the normal-sized (G) and big (H) cells sorted by flow cytometry. PCR amplification was performed as described in panel A.

SI Videos

Supplementary video 1. 3D reconstruction of a STSV2-infected REY15A cell in the process of asymmetric cell division by budding. The cells were stained with DAPI and observed using Leica SP8 immunofluorescence microscope. The images were analyzed by the Leica Application Suite X (LAS X) software and displayed in the Volume mode. The color scale indicates the Z-depth. The 3D video was obtained by rotation around Y-axis and then the X-axis with 1.5 times enlargement.

SI Table

Table S1. Strains and oligonucleotides used in this study.

Strains		
Strain	**Genotype**	**Source**
S. islandicus REY15A	Wide type	(6)
ΔC1C2	REY15A *ΔpyrEF ΔlacS Δcrispr1 Δcrispr2*	(2)
Sis/pSeSD-CdvAΔC	CdvAΔC over-expression	(3)
Sis/pSeSD-ESCRT-III ΔC	ESCRT-IIIΔC over-expression	(3)
Sis/pGE-CdvA	CdvA knockdown strain	(7)
Sis/pGE-ESCRT-III	ESCRT-III knockdown strain	(7)
Saccharomyces cerevisiae Y2H Gold	*MATa, trp1-901, leu2-3, 112, ura3-52, his3-200, gal4Δ, gal80Δ, LYS2 : : GAL1UAS-Gal1TATA-His3, GAL2UAS-Gal2TATA-Ade2 URA3 : : MEL1UAS-Mel1TATA AUR1-C MEL1*	Clontech
S1	REY15A clone 1 with CRISPR spacers against STSV2	This study
S2	REY15A clone 2 with CRISPR spacers against STSV2	This study
S3	REY15A clone 3 with CRISPR spacers against STSV2	This study
Oligonucleotides		
Name	**Sequence (5'-3')**	**Source**
16S-F	GAATGGGGGTGATACTGTCG	(8)
16S-R	TTTACAGCCGGGACTACAGG	(8)
Locus1-F	GTCCATAGGAGGACCAGC	(9)
Locus1-R	CCAACCCCTTAGTTCCTCCTC	(9)
Locus2-F	GTTCCTTCCACTATGGGACTA	(9)
Locus2-R	CGTCACTGACACCATATTTAT	(9)
STSV2_37-F	CTTCAGATCCAGTAAGAAGAG	This study
STSV2_37-R	GTGGTAATGCTGTACTGTTAG	This study
CdvA-F	GGTTCTTCTATCTTGACTATGG	This study
CdvA-R	GTATAATTCCTCTAACGCTCTC	This study
ESCRT-III-F	GTAGTTCCTGCGGTAGTAG	This study
ESCRT-III-R	CTTGACGATTGCTCTATTGG	This study
Vps4-S-F	CCAGAATCAGTAGCGAGAAC	This study
Vps4-S-R	AGTTGTACCATCTCCTCCAC	This study
ESCRT-III-1-F	GCTCCATGATTAGTAGGCTTG	This study
ESCRT-III-1-R	CTGCTACCTCATTAGCGTAC	This study
ESCRT-III-2-F	GGTCGTAGAATCTCAGATGTC	This study
ESCRT-III-2-R	CTGAGTTGTACTTGCTCTAGG	This study
ESCRT-III-3-F	GCTGAGCTGCTAATAGACG	This study
ESCRT-III-3-R	CTCAGACTCTCTAGCAACC	This study
TBP-F	GTGGCAACAGTTACGTTAGAG	This study
TBP-R	CCTTGGGCTGTTCTAATCTG	This study

SI References

1. Uldahl KB, Walk ST, Olshefsky SC, Young MJ, & Peng X (2017) SMV1, an extremely stable thermophilic virus platform for nanoparticle trafficking in the mammalian GI tract. *J Appl Microbiol* 123(5):1286-1297.
2. Gudbergsdottir S*, et al.* (2011) Dynamic properties of the Sulfolobus CRISPR/Cas and CRISPR/Cmr systems when challenged with vector-borne viral and plasmid genes and protospacers. *Mol Microbiol* 79(1):35-49.
3. Liu J*, et al.* (2017) Functional assignment of multiple ESCRT-III homologs in cell division and budding in Sulfolobus islandicus. *Mol Microbiol* 105(4):540-553.
4. Zhang C*, et al.* (2019) Cell Structure Changes in the Hyperthermophilic Crenarchaeon Sulfolobus islandicus Lacking the S-Layer. *mBio* 10(4):e01589-01519.
5. Schmittgen TD & Livak KJ (2008) Analyzing real-time PCR data by the comparative C(T) method. *Nat Protoc* 3(6):1101-1108.
6. Guo L*, et al.* (2011) Genome analyses of Icelandic strains of Sulfolobus islandicus, model organisms for genetic and virus-host interaction studies. *J Bacteriol* 193(7):1672-1680.
7. Liu J*, et al.* (2021) Archaeal extracellular vesicles are produced in an ESCRT-dependent manner and promote gene transfer and nutrient cycling in extreme environments. *bioRxiv* doi: https://doi.org/10.1101/2021.02.09.430445.
8. Sun M*, et al.* (2018) An Orc1/Cdc6 ortholog functions as a key regulator in the DNA damage response in Archaea. *Nucleic Acids Res* 46(13):6697-6711.
9. Erdmann S*, et al.* (2014) A novel single-tailed fusiform Sulfolobus virus STSV2 infecting model Sulfolobus species. *Extremophiles* 18(1):51-60.